Germanium and InGaAs/InP SPADs
for Single-Photon Detection in the Near-Infrared

Alberto Tosi[*], Alberto Dalla Mora, Franco Zappa, Sergio Cova
Politecnico di Milano – DEI, Piazza Leonardo da Vinci 32 - 20133 Milano, Italy

ABSTRACT

Single-Photon Avalanche Diodes (SPADs) for near-infrared (800-1700 nm) wavelengths can be manufactured both in InGaAs/InP and in germanium. Recently, new InGaAs/InP SPADs became commercially available with good overall performances, but with the intrinsic bottleneck of strong afterpulsing effect, originated in the InP multiplication layer. At present, germanium technology is not exploited for single-photon detectors, but previous devices demonstrate lower afterpulsing even at very low temperatures and promising dark count rate when employing pure manufacturing process. In this work, we compare germanium and InGaAs/InP SPADs in terms of dark counts, afterpulsing, timing jitter, and quantum efficiency. Eventually, we highlight the motivations for considering germanium as a key material for single-photon counting in the NIR.

Keywords: Single Photon Counting, TCSPC, Photon Timing, Single Photon Detector, Active Quenching, Gated Detector, Infrared Photons, Afterpulsing, Dark Count Rate, Time jitter.

1. INTRODUCTION

Many applications require high-efficiency, low-noise, high count-rate single-photon detectors in the near-infrared (NIR) wavelength range (800-1700 nm).

Nowadays, secure communication is an essential need for companies, public institutions and also individual citizens. Quantum cryptography is a technology that is provably secure against arbitrary computing power, and even against quantum computer attacks. It is based on Quantum Key Distribution (QKD) that allows two remote parties to generate a secret key, with privacy guaranteed by quantum mechanics [1]. The physical layer is made of single-photon sources, optical fibers and single-photon detectors at 1550 nm. A key requirement is the ability to operate the single-photon detector in nanosecond time-slots at high frequency in order to generate secret keys at high rates.

By exploiting the spontaneous photon emission of switching MOSFETs, the Picosecond Imaging for Circuit Analysis (PICA) and the Time-Resolved Emission (TRE) techniques [2] test and debug ULSI circuits in a non-invasive optical way. In order to non-invasively characterize digital and analog signals in scaled technologies, high sensitivity (in the 800-1500 nm range) and picosecond resolution are needed. In contrast to QKD, this application requires to gate-on the photodetector for long time intervals, even more than 100 ns, and to provide high quantum efficiency over a broad spectrum (1000-1600 nm).

Single-photon detectors are used also to measure the distance of an object, by means of three-dimensional (3D) eye-safe laser ranging (Light Detection and Ranging, LIDAR), thus featuring few-centimeter range resolution [3]. LIDAR main requirements are high sensitivity and low time-jitter detectors.

Optical Time Domain Reflectometry (OTDR) is the most widely used fiber-test method. When employing photon counting techniques, OTDR reaches spatial resolution as short as few centimeters [4].

Among other applications that benefit from photon-counting techniques in the NIR wavelength band, there are Raman light detection for fluorescence-free trace-gas detection, singlet oxygen detection for photodynamic therapy (PDT) dosimetry, time-resolved spectroscopy and other fluorescence decay analysis.

Different technologies for single-photon detectors are available: PhotoMultiplier Tubes (PMT), Superconducting Single-Photon Detectors (SSPD), Single-Photon Avalanche Diodes (SPAD).

---

[*] alberto.tosi@polimi.it; phone +39-02-2399-6174; fax +39-02-2399-3699

PMTs exploit the internal electron multiplication process (cascaded secondary electron emissions in vacuum) and attain internal gain of about 10^6, hence in response to single-photons they produce electrical signals well above the noise of the readout electronics.

The SSPD intrinsically has quantum nature and low noise when operate at extreme cryogenic temperatures (2.4 K) [5]. The SSPD has low time-jitter (30 ps) and is capable of high count rates (in the GHz range), but the active area is small (10 μm × 10 μm) and it requires bulky cryostats. Such detrimental characteristics make it unpractical for many single photon applications.

Semiconductor APDs have the typical advantages of solid state devices (small size, low bias voltage, low power consumption, ruggedness and reliability, etc.). In APDs operating in linear mode, the internal gain is not sufficient to detect single photons. Instead, single photons can be efficiently detected by avalanche diodes operating in Geiger-mode, known as Single-Photon Avalanche Diode (SPAD).

The SPAD detector is a p-n junction, operated in reverse-biased above the breakdown voltage, V_B, in order to exploit the fast and intense avalanche build-up triggered by the absorption of a single photon. In fact, the absorption of a photon generates an electron-hole pair in the high electric-field depleted region. Depending on the SPAD design, one or both photo-generated carriers impact ionize and ignite a multiplication process. Since the bias voltage exceeds the breakdown voltage, a self-sustained current builds up in the milliampere range. The sub-nanosecond rise of the avalanche current marks with high precision the photon arrival-time. A suitable circuit associated to the photodiode senses the avalanche, quenches it by lowering the voltage below the breakdown level, and finally resets the voltage above breakdown to the quiescent level, in order to make the detector ready to be ignited by another photon [6].

A proper process design and high quality fabrication steps enable the SPAD to be biased above V_B and stay in a zero-current state for a sufficiently long time (from some microseconds to seconds), while waiting for photons. In such operation mode (often called Geiger-mode) the photodiode is an "opto-electrical flip-flop": the detector is set when a single photon is absorbed and the photo-generated carriers succeed in triggering the avalanche process; the following electronics easily senses the current pulse and produces a standard high level voltage pulse; the detector is finally reset either by means of a high-value series resistance (passive self-quenching of the avalanche process) or by a more complex electronics (active quenching and active reset).

Silicon SPADs have been extensively investigated and are nowadays well known and employed. Considerable progress has been achieved in design and fabrication techniques and devices with good characteristics are commercially available [7] [8]. On the contrary, germanium and InGaAs/InP SPADs are not well developed yet. The manufacturing technology is not as advanced as the silicon one and their internal structures have to be optimized.

2. GERMANIUM AND INGAAS/INP SPADS

The first near-infrared SPADs were commercially available APDs designed for fiber communications that were operated in Geiger-mode [9] [10]. Germanium and $In_{0.53}Ga_{0.47}As$/InP APDs exploit the narrow bandgap in order to absorb near-infrared photons. The drawback is a higher thermal generation of carriers than in silicon. Hence, for reducing the dark count rate (DCR) to tolerable levels, devices must be cooled well below room temperature.

A germanium avalanche diode is usually a planar abrupt p^+n junction that, in order to avoid edge-breakdown and microplasmas, employs guard rings (i.e., regions of high breakdown voltage surrounding the active area) or mesa structures (see Fig. 1). Since the band-gap is small and the electric field is high (when operated in Geiger-mode), the electron-hole pair generation in dark condition is strong. High-purity materials, uniform doping concentrations and low dislocation density help to keep dark counts at low levels. However, germanium devices require deep cooling down to liquid nitrogen temperature (77 K) or lower. At those low temperatures the detection efficiency at 1550 nm is significantly reduced due to the bandgap broadening. The poor performance in fiber-based application limited the development of germanium detectors. Nevertheless, a good germanium technology could produce high performance photodetectors for NIR single-photon counting applications.

Thanks to the separate absorption and multiplication (SAM) structure, moderate cooling is sufficient for InGaAs/InP devices, which can operate in the range from 150 K to 220 K and provide good photon detection efficiency (more than 30%) up to 1.7 μm. InGaAs SPADs are based on materials and structures similar to those used for APDs. In fact many
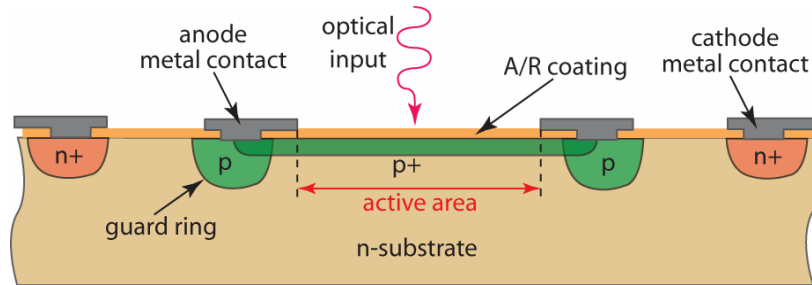
Fig. 1 Typical germanium APD cross-section. Note the guard ring for increasing the edge breakdown voltage.

attempts were reported with state-of-the-art commercially-available linear-mode APDs, employed as SPADs, after careful sample selection. However there is substantial room for improvements, since the optimization of InGaAs/InP structures for SPADs requires design approaches that are quite distinct from those proved effective for linear-mode APDs. Their noise is mainly determined by the shot-noise associated with leakage or dark currents. In contrast, SPAD suffers from false counts (the so-called dark counts) that arise when carriers are created by processes other than photon absorption, like thermal excitation and field-assisted generation of free carriers (i.e., tunneling processes).

The InGaAs/InP avalanche photodetector shown in Fig. 2 [11] contains an absorption layer of $In_{0.53}Ga_{0.47}As$ ($E_g \sim 0.75$ eV at 295 K) used to absorb photons with the wavelength of interest (800-1700 nm), lattice-matched to the InP substrate. The top InP region (with wider bandgap $E_g \sim 1.35$ eV) is where avalanche multiplication occurs (Fig. 2). When designing linear mode InGaAs/InP APDs, an optimal electric field profile should be tailored below breakdown at modest gains of 10-20, in order to achieve maximum signal-to-noise ratio. For SPADs intended for operation above breakdown, the electric field profile should be optimized for operation at the target reversed biased. Therefore, primary goal of InGaAs SPAD design is to maintain low electric field in the narrow bandgap absorber (to avoid tunneling) while attaining sufficiently high electric field in the multiplication region (to boost impact ionization, i.e. avalanche multiplication). The inclusion of a charged layer between absorption and multiplication regions allows for flexible tailoring of the internal electric field profile [11]. The addition of grading layers between InGaAs and InP is important to reduce carrier (specifically hole) pile-up effects, which result from the valence band offset that arises in an abrupt InGaAs/InP heterojunction [13]. In particular, the total field control charge should be larger in a SPAD than in a linear mode APD, in order to maintain low field intensity in the absorption region while standing a higher field in the multiplication region for Geiger-mode operation.
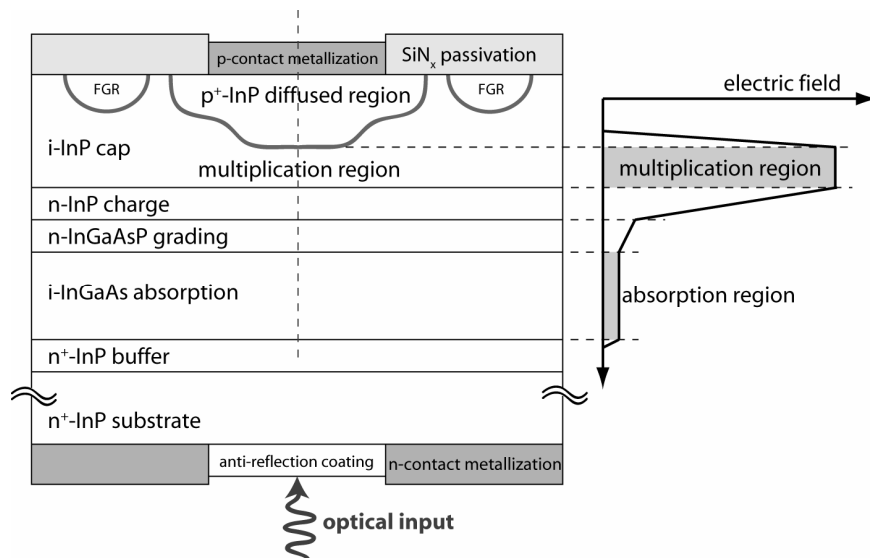

Fig. 2 Typical InGaAs/InP SPAD cross-section and related electric field profile.

In the cross-section shown in Fig. 2, the active area is defined by a p+ Zn diffusion into the top intrinsically-doped InP layer. The zinc dopant is introduced through a patterned SiN dielectric passivation layer, which acts as a diffusion mask. A single-step quasi-cylindrical junction would exhibit a deleterious electric field enhancement where the junction curvature is maximum, which leads to premature avalanche breakdown at the edges of the diffusion. For this reason two-step diffusion is employed [14]: the central deeper junction defines the active area, where the electric field peaks and the InGaAs absorption layer is depleted; while the shallow peripheral diffusion guarantees a lower electric field around the active area. The latter effect helps in reducing the reverse leakage current from the device bulk. Furthermore at the neighborhood of the active area, floating guard rings (FGRs) guarantee low peripheral leakage and further help avoiding edge breakdown.

In the following section we compare germanium and $In_{0.53}Ga_{0.47}As/InP$ SPADs, in terms of dark counts, afterpulsing, time jitter and photon-detection efficiency, in order to highlight that germanium detectors could be better than InGaAs/InP ones for many applications demanding high count rates.

3. EXPERIMENTAL SETUP

We compared commercially-available Germanium APDs, operated in Geiger-mode, with InGaAs/InP SPAD devices. While the latter were explicitly designed as SPADs, with an electric field profile engineered for operation above the breakdown voltage, Germanium APDs were not optimized.

In Geiger mode an avalanche photodiode can work either in free-running or in gated regime. In the former case an external circuit senses the onset of the avalanche current, generates a standard output pulse, and quenches the avalanche, by lowering the bias below breakdown. After a defined time interval, the diode bias is restored to the operating value. However, the avalanche rate is due not only to photon absorption but also to dark counts, i.e. carriers generated by thermal, tunneling, and trapping processes inside the semiconductor. NIR SPADs have dark count rates higher than silicon ones, also at low temperatures, ruling out free-running operation because most of the counting dynamics is spoiled by dark counts. Nevertheless, gated-mode is feasible.

We performed the measurements herein reported by means of a gated quenching circuit. In quiescence, the photodetector is biased 0.5 V below the breakdown voltage for most of the time (T_{OFF}). Then the reverse voltage is raised above breakdown for a short gate-on time T_{ON}. Fig. 3 shows the gate pulse, with a gate frequency $f_{GATE} = 1/(T_{ON}+T_{OFF})$. The excess bias V_{EX} is the difference between bias voltage V_{BIAS} and breakdown voltage V_B, i.e. $V_{EX} = V_{BIAS} - V_B$.

The SPAD avalanche rate is measured by an external counter, which provides the number ($n_{COUNTER}$) of avalanche pulses per second. Since the photodetector works in gated-mode regime, it is enabled for a small percentage of the measurement time, equal to $T_{ON}/(T_{ON}+T_{OFF})$. Therefore, the dark count rate (DCR) could be estimated as:

$$\frac{n_{COUNTER}}{T_{ON} \cdot f_{GATE}} \tag{1}$$

But, at high count rates more than one photon could be absorbed within every gate-on time interval, although only the first will trigger the SPAD and will be detected. Thus the correct count rate can be properly estimated taking into account Poisson statistics. The result is that the estimated count rate $n_{ESTIMATED}$ is higher:

$$n_{ESTIMATED} = -f_{GATE} \cdot \ln\left(1 - \frac{n_{COUNTER}}{f_{GATE}}\right) \tag{2}$$

and eventually

$$DCR = \frac{n_{ESTIMATED}}{T_{ON} \cdot f_{GATE}} = -\frac{1}{T_{ON}} \cdot \ln\left(1 - \frac{n_{COUNTER}}{f_{GATE}}\right). \tag{3}$$
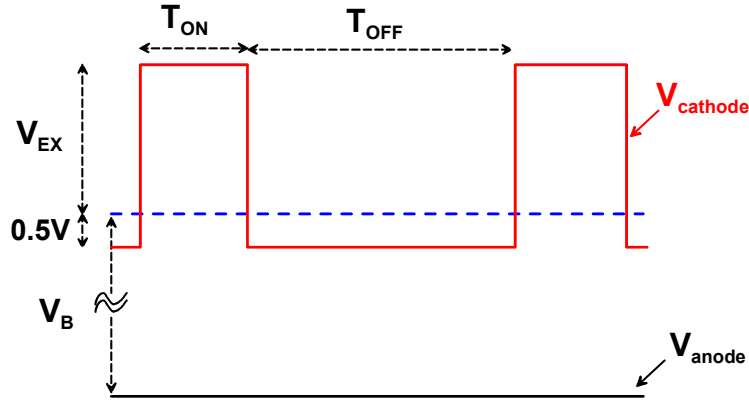
Fig. 3 Gating pulse ($V_{cathode}$) for biasing the SPAD above the breakdown level (V_B), compared to the DC anode voltage (V_{anode}).
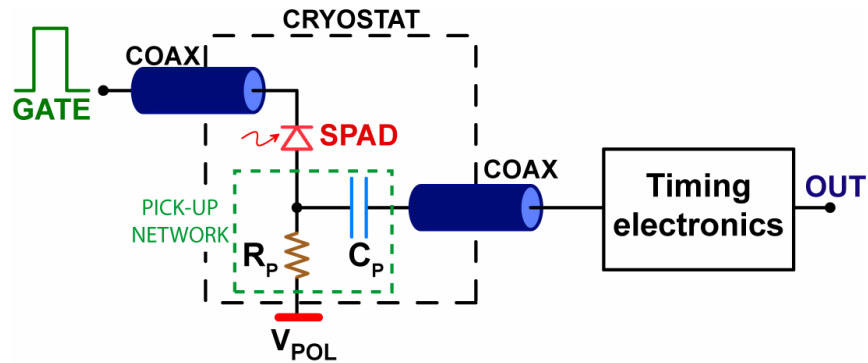

Fig. 4 Experimental setup for germanium and InGaAs SPAD characterization.

The devices were mounted inside a closed-cycle helium-gas cryostat as shown in Fig. 4. We generated the gate-on pulse with a standard pulse generator and we fed it directly to the cathode pin of the SPAD through a 50-Ω coaxial cable (with appropriate termination). In quiescence, the cathode was biased at 0 V and then it was risen by the gate-on signal. The rising- and falling-edges were faster than 3 ns, while the gate-on time-slot lasts T_{ON} = 20 ns, unless otherwise reported. The anode potential was kept at a negative level through a ballast resistor, in order to bias the photodetector in quiescence 0.5 V below breakdown. The output signal was sensed through a coupling capacitor from the SPAD anode and fed through a 50-Ω coaxial cable to the counting and timing electronics.

4. PRIMARY DARK COUNT RATE

The primary source of SPAD noise is due to carriers either thermally generated or emitted by tunneling processes. Then another contribution adds, due to the release (*afterpulsing*) of carriers, trapped during previous avalanche ignitions. In order to assess the contribution of thermal generation and tunneling, trapped carriers must be completely released between two subsequent enabling of the detector. For this reason, we employed a fixed gate-on duration (T_{ON} = 20 ns) and a very long gate-off period (T_{OFF} = 1 ms, i.e. f_{GATE} = 1 kHz), which allows a complete release of trapped carriers, thus avoiding afterpulsing effects.

We characterized two different germanium avalanche photodiodes, the GAV40 APD from GPD Optoelectronics [15] (40-μm diameter, V_B = 19 V at 77 K) and the GA-1U APD from Texas Instruments (TI) [16] (350-μm diameter, V_B = 29 V at 77 K).
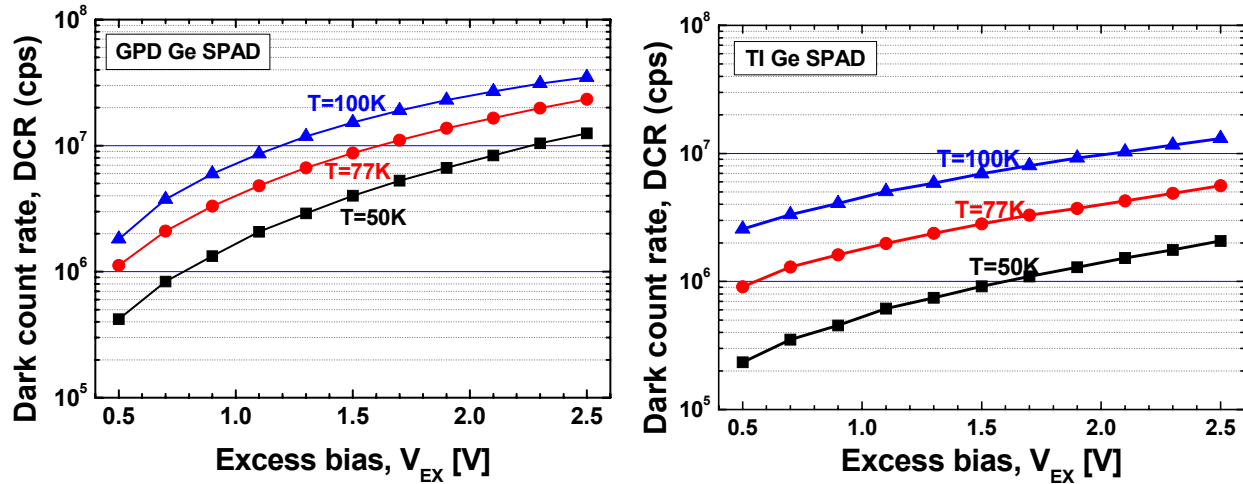
Fig. 5 Dark count rate depends almost exponentially on excess bias: 40-μm GPD diode (left) and 350-μm Texas Instruments diode (right) operated in gated-mode at 1 kHz with T_{ON} = 20 ns.
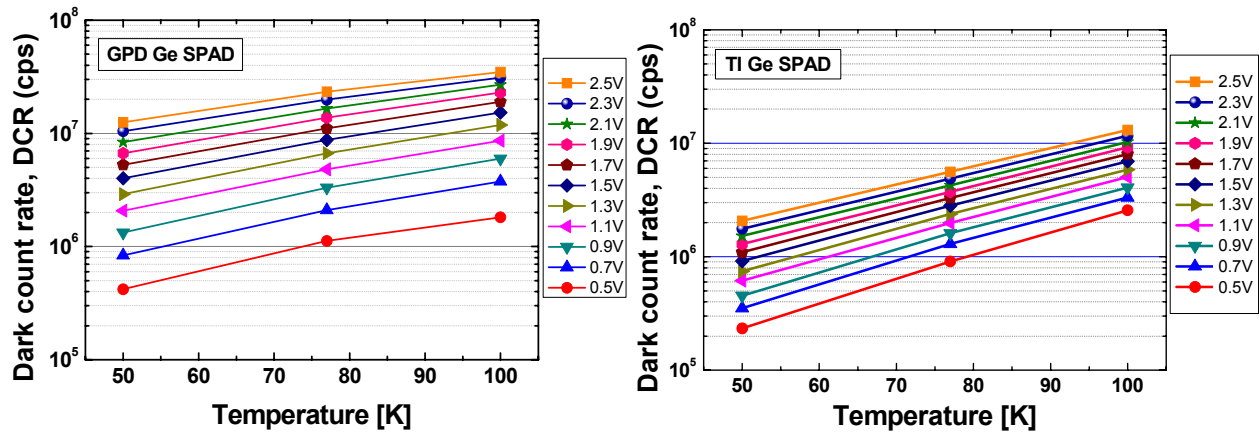

Fig. 6 Dark count rate vs. temperature at different excess biases: GPD diode (left) and Texas Instruments diode (right) operated in gated-mode at 1 kHz with T_{ON} = 20 ns.

Thermal generation in GPD devices is quite high at all temperatures (Fig. 5 left and Fig. 6 left). For instance at 77 K, DCR is about 1 Mcps (i.e. mega counts per second) at an excess bias of 0.5 V, and it is more than 8 Mcps at an excess bias of 1.5 V. At 50 K, the DCR is halved, being about 500 kHz at 0.5 V and 4 Mcps at 1.5 V excess bias (Fig. 5 left).

Texas Instruments avalanche photodiodes have lower DCR (Fig. 5 right and Fig. 6 right), e.g. 700 kcps at an excess bias of 0.5 V, and 3 Mcps at an excess bias of 1.5 V. At 50 K Texas Instruments devices have 250 kcps and 1 Mcps at 0.5 V and 1.5 V of excess bias (see Fig. 5 right).

In order to fairly compare the quality of the two technologies, we computed the DCR densities, i.e. DCR per unit active area (cps/μm^2), and then their ratio:

$$\frac{DCR_{GPD}/(40\mu m)^2}{DCR_{TI}/(350\mu m)^2} \sim= 220 \tag{4}$$

A better comparison should be computed on the DCRs per unit volume (μm^{-3}). We extrapolated the depletion layer thicknesses by assuming simple abrupt step-junction and uniform doping. In this way, we obtained a thickness of 3.8 μm and 5.8 μm for GPD and Texas Instrument device, respectively. Therefore, the DCR per unit of volume leads to a ratio:

$$\frac{DCR_{GPD}\big|_{\text{unit volume}}}{DCR_{TI}\big|_{\text{unit volume}}} \sim= 350 \ . \tag{5}$$

This clearly shows that Texas Instruments' fabrication process introduces less lattice defects than the GPD one, thus yielding a much lower dark count rate. Unfortunately, Texas Instruments diodes have too large an active area (350 μm diameter) and, therefore, the total dark count rate is high.

Thanks to the SAM structure, InGaAs/InP SPADs have a lower electric field in the narrow-bandgap absorption layer, which helps to keep tunnel generation at low levels and, eventually, to reduce dark current generation. Hence, if thermal generation rates are comparable, InGaAs SPADs should have a primary DCR lower than the germanium one because of lower tunneling.

We investigated the performance of several InGaAs APDs from different suppliers and the SPADs from Princeton Lightwave (PLI) (40-μm diameter active area, $V_B = 39$ V at 200 K) [7] will be used in the following as a reference when comparing germanium to InGaAs devices. Such comparison is not straightforward since the operating conditions are quite different. The typical operating temperatures of germanium devices is 77 K with an excess bias of about 1.5 V, while InGaAs SPADs works at higher temperatures, typically around 200 K, with an excess bias of about 5 V.

If we compare commercially available devices, such as GPD germanium APD and PLI InGaAs APD, both with a diameter of 40 μm, it results that the DCR of InGaAs is roughly two orders of magnitude lower ($\sim$ 280 times).

However, by comparing the DCR density of Texas Instruments germanium APD vs. PLI InGaAs APD one, it results that

$$\frac{DCR_{TI}\big/(350\mu m)^2}{DCR_{PLI}\big/(40\mu m)^2} \sim= 1 \ . \tag{6}$$

If a 40-μm germanium SPAD manufactured with the same technology of the Texas Instruments 350 μm APD were available, it would result in a single-photon detector with sufficiently low dark count rate (at 77 K and 1.5-V excess bias) to be comparable with commercially available InGaAs SPADs (at 200 K and 5-V excess bias).
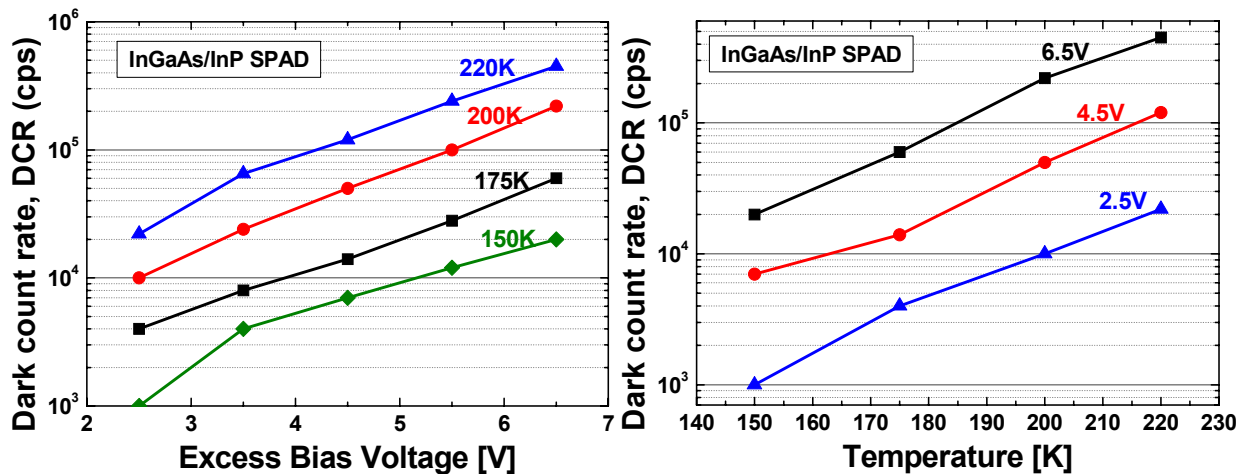

Fig. 7 Dependence of primary dark count rate on the excess bias (left) and on temperature (right) of an InGaAs/InP SPAD by Princeton Lightwave (PLI) [7], with 40 μm diameter, operated in gated-mode at 1 kHz with T_{ON} = 50 ns.

5. AFTERPULSING

If the dark count rate were due only to primary dark counts, the total measurable DCR would not depend on the gating frequency. On the other hand, experimental results reported in Fig. 8 and Fig. 9 show that the dark count rate increases as T_{OFF} decreases (i.e. when the gate frequency f_{GATE} increases). This effect is named *afterpulsing* [17] [18] and is due to the capture and the delayed release of avalanche carriers through deep levels.

In SPAD devices, during the avalanche process there are high concentrations of carriers (both electrons and holes) in the multiplication region. Both carriers can be trapped into deep levels: delayed release of trapped carriers can re-trigger the avalanche, thus remarkably increasing the total photodetector dark-count rate. The effect introduces a secondary source of dark counts, with a carrier generation rate proportional to the population of trap levels. Unluckily, these levels have fairly high concentrations and fairly long lifetimes. The release time constants are longer than microseconds for germanium devices and tens of microseconds for InGaAs devices, and remarkably increase as the temperature lowers. The long lifetime causes the trap population to build up in successive avalanche pulses, thereby increasing the total DCR by orders of magnitude. In GPD devices, with repetition rates between 1 kHz and 250 kHz (*i.e.* with T_{OFF} ranging from 1 ms to 4 µs), we noticed no significant increase of the DCR with excess biases $V_{EX} \leq 1.5$ V. This means that release time constants are shorter than 4 µs (Fig. 8). Such behavior is better than what we measured in InGaAs/InP detectors, which show time constants of tens of µs even at relatively high temperatures (Fig. 9).

On the basis of our measurements, we conclude that trap-release time-constants are quite different in germanium and InGaAs devices. In detail, germanium SPADs have time constants in the order of microseconds at 77 K, while InGaAs SPADs have time constants in the order of tens of microseconds at 200 K. Therefore, in order to keep the primary DCR low, germanium devices should be operated inside liquid nitrogen dewars, while not being overwhelmed by afterpulsing.

Trap population increases during an avalanche pulse, proportionally to the total flowing avalanche charge [6]. Indeed at longer T_{ON} windows, more charge flows and gets trapped thus boosting afterpulsing [6], i.e. the DCR levels. Therefore, in cases where the photon arrival time is precisely defined (for instance, in QKD systems) the afterpulsing can be strongly reduced by employing a very short T_{ON}, of just 1 ns. In other applications, longer T_{ON} must be employed (from tens to hundreds of ns) [2] and, therefore, the usual gated passive quenching would lead to strong afterpulsing. Such drawback can be avoided by employing a gated active quenching circuit (AQC) [6], which quenches the avalanche current a few nanoseconds after triggering, without waiting the end of the gate-on interval. The advantage is lower trapped population in comparison to the simple gate quenching, i.e. reduced afterpulsing.
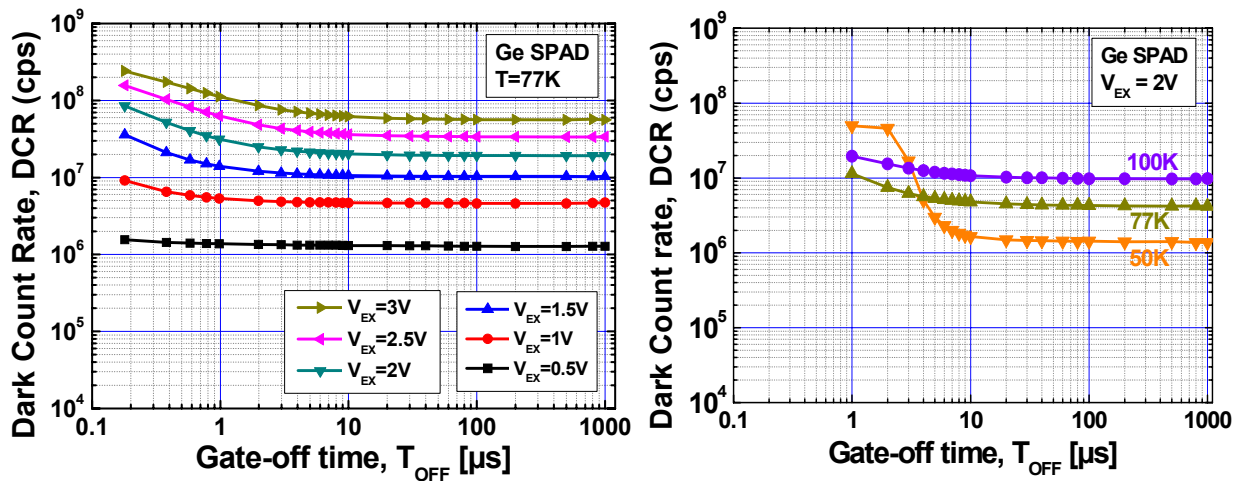

Fig. 8 Dark count rate of germanium GPD (left) and TI (right) SPADs measured at various excess biases and temperatures in gated operation (T_{ON} = 20 ns) as a function of the idle interval T_{OFF}. The primary DCR is the count rate reached at sufficiently long T_{OFF}, when afterpulsing plays a negligible role and the DCR flattens.
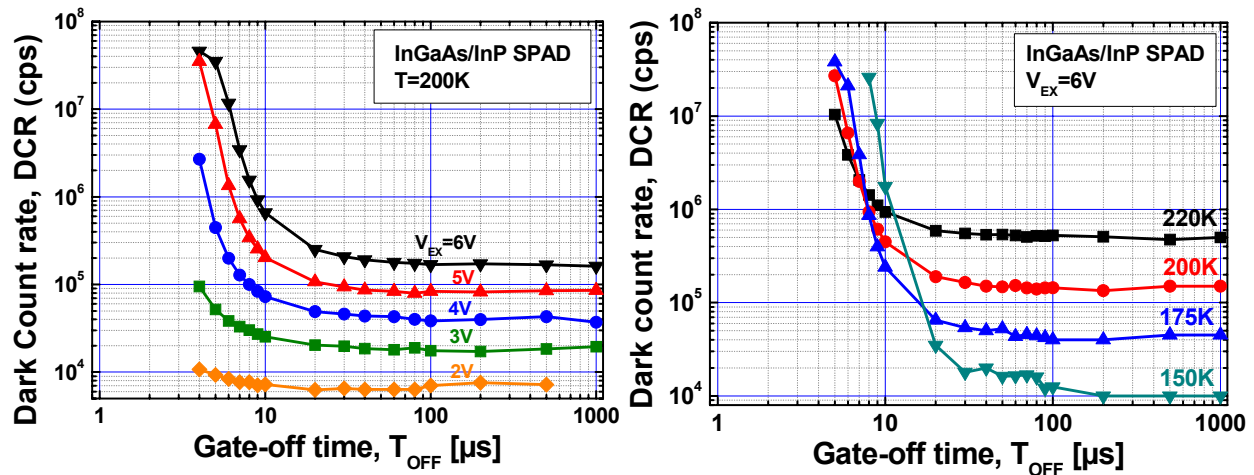
Fig. 9 Dark count rate of InGaAs PLI SPAD measured at various excess biases (left) and temperatures (right) in gated operation (T_{ON} = 20 ns) as a function of the idle interval T_{OFF}. The primary DCR is the count rate reached at sufficiently long T_{OFF}, when afterpulsing plays a negligible role and the DCR flattens.

6. TIMING JITTER

In order to attain high resolution in photon timing, the electronic circuit should extract the time information from the very first part of the avalanche build-up [19]. We devised a simple approach to overcome this limitation: a R_P-C_P pick-up network for sensing the fast avalanche current signal from the SPAD anode, while connecting the pulse generator directly to the cathode (see Fig. 4). The pick-up circuit extracts a fast rising signal and feeds it to the timing electronics.

The fast rising- and falling-edges of the gate signal (in the order of 10 V/ns or faster) generate capacitance feed-throughs that result in "spurious" spikes at the comparator input. Therefore, in order to detect only the avalanche pulse, the threshold of the sensing comparator should be set to high values, thus deteriorating the timing performance [19]. It is even very common that spurious peaks are higher than avalanche pulses, thus making avalanche detection challenging. We solved the problem by introducing a compensation signal obtained by means of a parallel capacitive path that generates a "dummy" signal that mimics only the feed-through spikes [20]. The SPAD signal (spurious spikes and avalanche pulse) and the dummy path signal (spikes only) are fed to the two inputs of a custom differential comparator. The latter senses the difference between the two signals (i.e. just the avalanche pulse) and correctly detects the photon arrival.

We ascertained the timing performance of germanium and InGaAs/InP SPADs at different temperatures and excess biases. Higher excess bias help obtaining faster triggering of the electronics, with a corresponding reduction of timing jitter. We characterized the timing jitter of the GPD device at 77 K, by means of a pulsed laser at 1.3-μm wavelength and with a pulse width of 40 ps_{FWHM} (Full Width at Half Maximum). In all measurements we set f_{GATE} = 10 kHz. The timing performance is quite good, since we measured pulsed widths (including the laser pulse width) narrower than 100 ps_{FWHM} at excess biases of 1.5-2 V (Fig. 10 left). Such timing performances are better than those we measured with the Texas Instruments device, which range from 100 ps to 150 ps at excess biases of 1.5-2 V. The negligible difference in time jitter may be due to the difference in active area dimensions.

We experimentally characterized the time jitter of InGaAs SPADs by means of a 1550-nm pulsed laser with pulse width of about 20 ps_{FWHM}. We obtained a time resolution of about 46 ps_{FWHM} (Fig. 10 right). However, lower temperatures degrade timing performance, since the photo-generated hole piles up at the heterojunction, before igniting the avalanche, thus spoiling the timing resolution of the device (Fig. 11 right). The adoption of a grading InGaAsP quaternary layer can drastically minimize such effect, thus speeding up hole-collection into the high-field region and, eventually, avalanche current build-up. Instead, such detrimental effect is not present in germanium SPAD (Fig. 11 left).
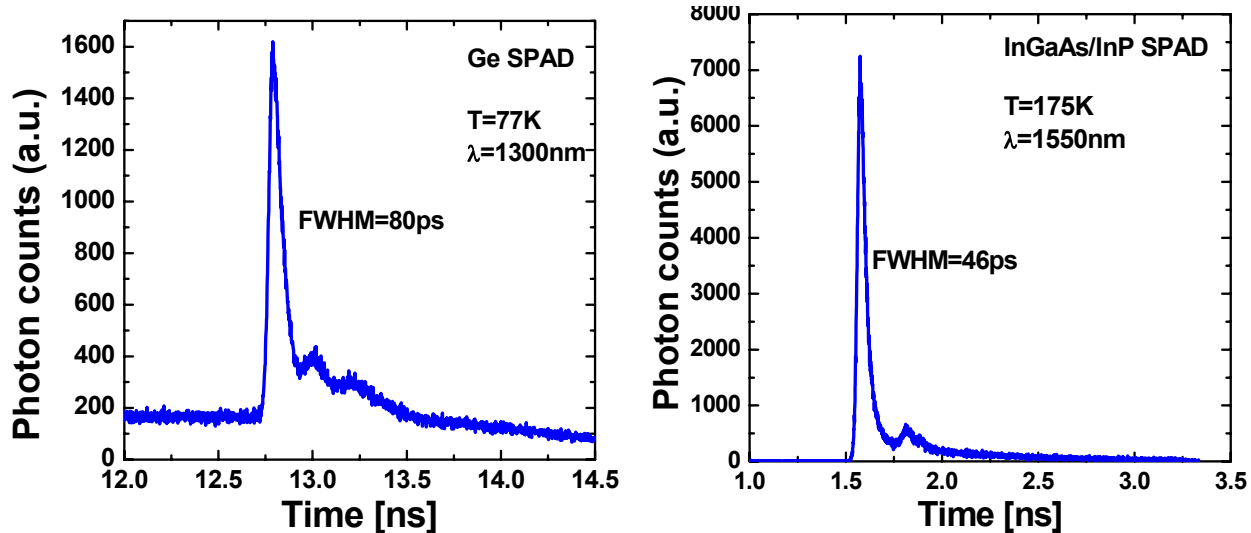
Fig. 10 Timing response of the germanium (left) and InGaAs (right) SPADs to laser pulses. The two trailing bumps are due to laser oscillations.
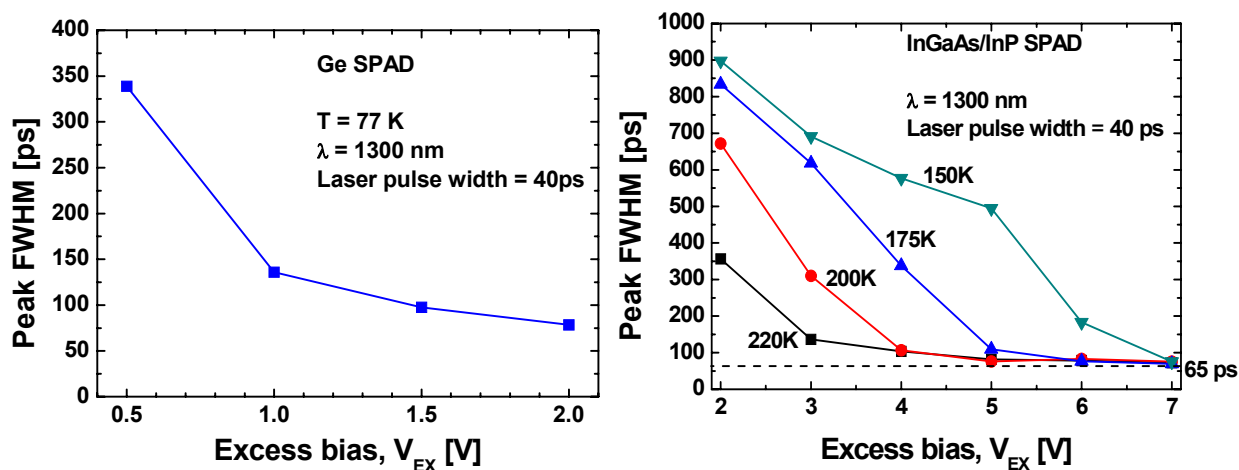

Fig. 11 Timing jitter of the germanium (left) InGaAs/InP (right) SPADs when illuminated by a 1300nm laser with 40ps pulse width.

7. PHOTON DETECTION EFFICIENCY

SPAD Photon Detection Efficiency (PDE) depends on the photon absorption probability, but not only on that. It also depends on the probability that the photo-generated carrier succeeds in triggering the self-sustaining avalanche process [21]. Therefore, it is equal to the product of the absorption probability and the avalanche triggering probability. The latter increases first linearly with the excess bias and then tends to saturate to 100%. High excess bias is also desirable for reducing the jitter in photon timing. However, there is a trade-off with DCR, which increases almost exponentially with excess bias, due to the enhancement of the tunnel-assisted carrier generation.

In order to avoid afterpulsing, we measured the detection efficiency with very low gate frequencies (1 kHz for InGaAs/InP SPADs and 10 kHz for germanium SPADs). We used attenuated 1.31 μm and 1.55 μm continuous wave lasers.
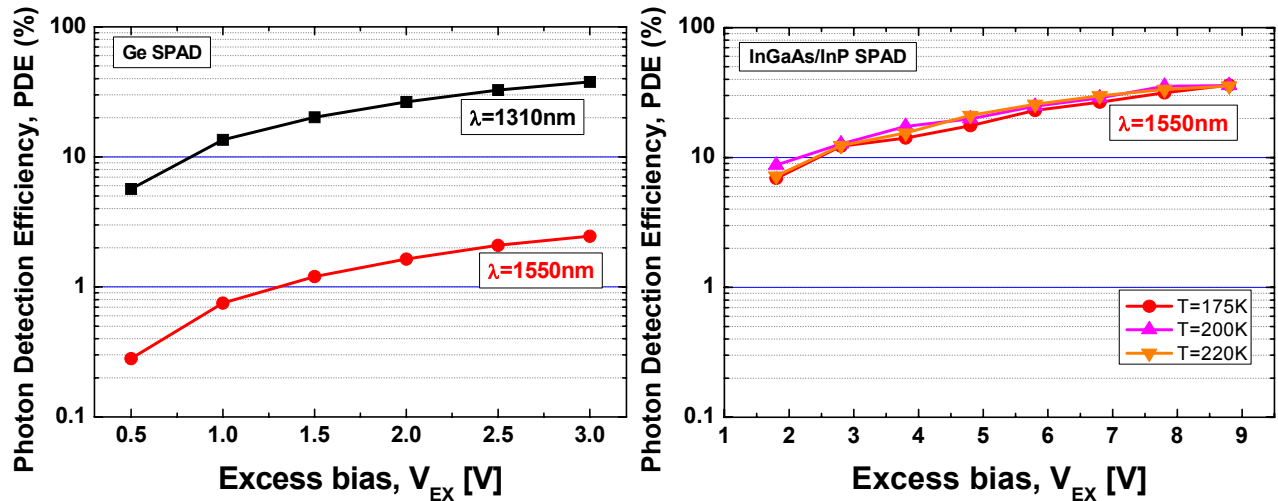
Fig. 12 Single Photon Detection Efficiency (PDE) of GPD germanium (left) and PLI InGaAs/InP SPADs at various excess biases.

We measured the PDE of InGaAs/InP SPADs at three temperatures (175 K, 200 K, and 220 K) at 1550 nm (Fig. 12 right). The obtained values are fairly good, ranging from 10 % at very low excess bias (below 3 V) to 35 % at high excess bias (above 8 V). We did not perform measurements at 1310 nm, but we expect higher PDE since the photon absorption probability is higher at 1310 nm than at 1550 nm.

It is well known that germanium devices have low PDE at 1550 nm, when cooled at cryogenic temperatures, therefore they have always been considered inadequate for single-photon detection at such wavelength. Nevertheless, we experimentally characterized germanium SPADs and at 77 K we obtained a PDE of about 30 % at 1310 nm (Fig. 12 left) and of about 1 % at 1550 nm. This proves that germanium SPADs can be profitably exploited not only at 1.3 μm but also for many other single-photon applications over a broader NIR wavelength.

8. CONCLUSIONS

In this paper we experimentally compared germanium and InGaAs/InP SPADs. We characterized the devices in terms of dark count rate, afterpulsing, timing jitter, and photon detection efficiency. The afterpulsing of germanium SPADs is lower than that of InGaAs/InP ones, even if germanium devices have to be operated at about 77 K, in order to keep dark count rates at low levels. Therefore, germanium SPADs can be operated at higher gate frequencies than InGaAs/InP ones, thus allowing a remarkable reduction of acquisition times. When comparing dark count rates, a good germanium technology (such as that employed by Texas Instruments) would result into a single-photon detector with sufficiently low dark count rate (at 77 K and 1.5-V excess bias), comparable to those of commercially available InGaAs/InP SPADs (at 200 K and 5-V excess bias). The timing performance of germanium SPAD is quite good, even if it is slightly worse than InGaAs/InP one. Finally, although the photon detection efficiency at 1550 nm of germanium SPAD is low, it shows good PDE at shorter wavelengths, making it a good choice for single-photon applications all over the 1-1.55 μm wavelength range.

REFERENCES

1. H. Zbinden, H. Bechmann-Pasquinucci, N. Gisin, and G. Ribordy, "Quantum Cryptography", Appl. Phys. B, vol. 67, 1998, pp. 743-748.
2. F. Stellari, A. Tosi, F. Zappa, and S. Cova, "CMOS Circuit Testing via Time-Resolved Luminescence Measurements and Simulations", Instrumentation and Measurement, IEEE Transactions on, Volume 53, Issue 1, Feb. 2004, pp. 163-169.

3.   U. Schreiber and C. Werner, "Laser radar ranging and atmospheric lidar techniques", Proceedings of SPIE, 3218, The International Society for Optical Engineering,1997.

4.   A. Lacaita, P. Francese, S. Cova, and G. Ripamonti, "Single-photon optical time-domain reflectometer at 1.3 μm with 5 cm resolution and high sensitivity", Optics Lett., 18, pp. 1110-1112 (1993).

5.   G. N. Gol'tsman, O. Okunev, G. Chulkova, A. Lipatov, A. Dzardanov, K. Smirnov, A. Semenov, B. Voronov, C. Williams, and R. Sobolewski, "Fabrication and properties of an ultrafast NbN hot-electron single-photon detector", IEEE Trans. On Applied Superconductivity, 11, pp. 574-577, 2001.

6.   S. Cova, M. Ghioni, A.L. Lacaita, C. Samori and F. Zappa, "Avalanche photodiodes and quenching circuits for single photon -detection", Appl. Opt. 35, 1956-1976 (1996).

7.   Princeton Lightwave Inc., www.princetonlightwave.com

8.   Sensors Unlimited Inc., www.sensorsinc.com

9.   A. Lacaita, F. Zappa, S. Cova, and P. Lovati, "Single-photon detection beyond 1 μm: performance of commercially available InGaAs/InP detectors", Appl. Opt., 35, 2986 (1996).

10. A. Lacaita, P.A. Francese, F. Zappa, and S. Cova, "Single photon detection beyond 1 μm: performance of commercially available germanium photodiodes", Appl. Opt. 33, 6902 (1994).

11. K. Nishida, K. Taguchi, and Y. Matsumoto, "InGaAsP heterostructure avalanche photodiodes with high avalanche gain," Appl. Phys. Lett., 35, 251–252 (1979).

12. J. C. Campbell, A. G. Dentai, W. S. Holden, and B. L. Kasper, "High-performance avalanche photodiode with separate absorption, 'grading', and multiplication regions," Electron. Lett., 19, 818 – 820 (1983).

13. S. R. Forrest, O. K. Kim, and R. G. Smith, "Optical response time of $In_{0.53}Ga_{0.47}As$ avalanche photodiodes," Appl. Phys. Lett., 41, 95–98 (1982).

14. Y. Liu, S. R. Forrest, J. Hladky, M. J. Lange, G. H. Olsen, D. E. Ackley, J. Lightwave Tech., 10, 182 (1992).

15. GPD optoelectronics, www.gpd-ir.com

16. Texas Instruments, www.ti.com

17. R. H. Haitz, "Mechanism contributing to the noise pulse rate of avalanche diodes", J. Appl. Phys., vol.36, 1965, pp. 3123-3131.

18. S. Cova, A.L. Lacaita, G. Ripamonti, 1991, IEEE Electron. Dev. Lett., 12, 685.

19. A. Gulinatti, P. Maccagnani, I. Rech, M. Ghioni and S. Cova, "35 ps time resolution at room temperature with large area single photon avalanche diodes", Electronics Letters 41, 272-274 (2005).

20. F. Zappa, A. Tosi and S. Cova "InGaAs SPAD and electronics for low time jitter and low noise," Proc. of SPIE Photon Counting Applications, Quantum Optics, and Quantum Cryptography, vol. 6583, no. 1, pp. 65830 2007.

21. W.O. Oldham, R.R. Samuelson and P. Antognetti, "Triggering Phenomena in Avalanche Diodes", IEEE Trans. Electron Devices ED-19, 1056-1060 (1972).